Journal of Applied Sciences

ISSN 1812-5654

science alert

ANSInet
an open access publisher
http://ansinet.com

Journal of Applied Sciences 12 (5): 492-497, 2012
ISSN 1812-5654 / DOI: 10.3923/jas.2012.492.497

An Axisymmetrical Finite Element Model for Prediction of the Bonding Behavior in HVOF Thermal Spraying Coatings

[1]Mahdi Jalali Azizpour, [2]Salman Norouzi and [1]D. Sajedipour
[1]Department of Mechanical Engineering, Ahwaz Branch, Islamic Azad University, Ahwaz, Iran
[2]Babol University of Technology, Babol, Iran

Abstract: The application of thermally sprayed coatings on metallic parts has been widely accepted as a solution to improve their mechanical and tribological properties. During High Velocity Oxy-Fuel (HVOF) thermal spraying, most particles remain in solid state prior to impact. An explicit axisymmetrical FE methodology is developed here to study the particle impingement and to establish the critical particle impact velocity needed for adequate bonding. Attention is focused on the prediction of bonding behavior for a WC-12Co HVOF sprayed coating on an AISI 1045 steel substrate. The numerical results indicate that in HVOF process the kinetic energy of the particle prior to impact plays the most dominant role on melting of the particle in interface region.

Key words: HVOF, FEM, WC-Co, bonding, critical velocity

INTRODUCTION

Thermally sprayed coatings are considered due to mechanical, metallurgical, tribological and magnetic properties. These properties are modified by selecting proper spray conditions or post heat treatment (Cherigui *et al*., 2007; Lyphout *et al*., 2008). Over the last years, the substitution of hard chromium plating has been promoted due to the new legislation concerned to hazardous wastes of Galvanic Industries. Thermal spray technology has been proposed as an alternative to hard chromium plating showing in some applications promising results. For instance, one requirement for tungsten carbide coatings is to have better wear and fatigue properties than hard chromium when applied in aircraft manufacturing (Sohi and Ghadami, 2010; Sahraoui *et al*., 2010). Thermal spray process is focused on repairing the damaged elements of pumps, turbines and compressors (Ahmad *et al*., 2007). Thermal spraying with high velocity oxygen fuel (Fig. 1) has been very successful in spraying wear resistant WC-Co coatings with higher density, superior bond strengths and less decarburization than many other thermal spray processes. This is attributed mainly to its high particle impact velocities and relatively low peak particle temperatures. As a class of hard composite material, WC-Co powder are widely used by various thermal spray processes to deposit protective coatings in a large variety of applications such as power plants, oil drilling, turning, cutting and milling, where abrasion, erosion and other forms of wear exist (Santana *et al*., 2008).

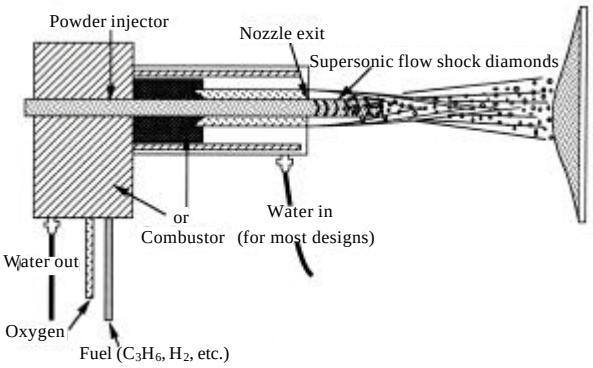

Fig. 1: High velocity oxy-fuel thermal spraying

The finite element method is widely used for the evaluation of mechanical property of machine elements such as residual stress and failure mechanism such as delaminating, fatigue behavior and Stress Intensity Factors for various types of crack configurations (Lyphout *et al*., 2008; Souiyah *et al*., 2009).

The adhesion strength of a coating depends on the bonding between the coating and substrate as well as on the coating microstructure. WC-Co particles, in general in range of 10-65 μm are fed into HVOF gun where they are heated and accelerated up to ultrasound velocities before impingement on the substrate surface (Sahraoui *et al*., 2010). Noticeable compressive stresses are generated in splat and substrate surface during the high velocity impact. The experimental observation (Gilmore *et al*., 1999; Li and Li, 2003; Kamnis and Gu, 2005; Kamnis *et al*., 2008) and numerical models of the deformation of solid particles

Corresponding Author: Mahdi Jalali Azizpour, Department of Mechanical Engineering, Ahwaz Branch, Islamic Azad University, Ahwaz, Iran

from cold spraying show that adhesion is a result of plastic deformation and related phenomena such as residual stress at the interface. Quantitative analyses on the relationship between the deposition efficiency and impact velocities of particles indicate a critical particle velocity for successful adhesion, i.e., particles below the critical velocity will rebound from the substrate only have abrasion and compressive residual stresses while particles above this critical velocity adhere on the previously lamellas and substrate (Dykhuizen *et al*., 1999; Karni *et al*., 2006; Grujicic *et al*., 2003).

In the present study, the development of an axisymmetrical finite element model is presented to simulate the bonding behavior in an HVOF sprayed particle. As such, the model can be used across a range of impact velocities and particle temperatures. The popular WC-Co powders are selected for this purpose. The WC-Co composite particle is considered as a single entity, with a single set of physical properties.

MATERIALS AND METHODS

The current work describes the development of an FE methodology to simulate the adhesion strength in HVOF sprayed coatings. For this purpose a two dimensional axisymmetric model of WC-12Co particle impacting on an AISI 1045 substrate disc was generated using ABAQUS version 6.10. A dynamic, explicit temperature-displacement coupled analysis was carried out to study the high strain-rate impact process using ABAQUS/Explicit which is outlined in next section. The WC solid nano-particles are dispersed in liquid Co phase during the flight. Temperatures in HVOF thermal spraying are not high enough to melt the tungsten carbide and therefore, the melting point for the primary material, cobalt, is applied in modeling of particle for the FEA analysis.

RESULTS AND DISCUSSION

Plasticity of impact: Impact of sprayed particles can also be treated as a high-temperature shot peening process. The impact of thermally sprayed particles onto a substrate is a non-linear dynamic contact phenomenon. The microscopic and macroscopic response of the impacting particle and the underlying substrate under such loading conditions is strongly affected by the strain, strain rate, temperature and microstructure of the material (Bansal *et al*., 2006).

Using an appropriate constitutive equation defining the material properties is therefore, essential for modeling such processes. The constitutive relation proposed by Johnson and Cook (1983) (the J-C model) is widely used in numerical models involving high strain rates and temperatures and its use is generally limited to the impact of solids. The J-C model is stated as follows (Johnson and Cook, 1983):

Table 1: J-C parameters of substrate

Model parameters J-C	AISI1045
A (MPa)	553.1
B (MPa)	600.8
N	0.234
C	0.013
M	1.0
Melting temp. (K)	1356
Reference strain rate (1 sec^{-1})	1.0

$$\bar{\sigma} = [A + B(\bar{\varepsilon}^{pl})^n][1 + C\ln(\frac{\dot{\bar{\varepsilon}}^{pl}}{\dot{\bar{\varepsilon}}_0})](1 - \hat{T}^m) \quad (1)$$

where, $\bar{\varepsilon}^{pl}$ is the equivalent plastic strain, $\dot{\bar{\varepsilon}}^{pl}$ is the equivalent plastic strain rate and A, B, C, m and n are material parameters and is the reference strain rate. $\hat{T}$ is a non-dimensional temperature, T_r room temperature and T_m is melting temperature:

$$\hat{T} = \frac{T - T_r}{T_m - T_r} \quad (2)$$

$$T = T_r + \frac{\beta}{\rho c_p}\int \bar{\sigma} d\bar{\varepsilon}_p \quad (3)$$

where, β is the work to heat conversion factor, c_p is the heat capacity and ρ is the density.

During impact, much of the kinetic energy of the particle will be transformed into heat. Hutchings (1981) argued that, during impact of a particle with a metal target during an erosion process, more than 80% of the original kinetic energy of the particle was transformed into heat, with the rest of the energy being accounted for by the stored energy of plastic deformation, the elastic wave energy and the rebound kinetic energy. In a more recent study of cold-spray deposition, it was assumed that 90% of the kinetic energy of the particle was dissipated into heat (Assadi *et al*., 2003).

Parameters of J-C model of AISI1045 substrate is shown in Table 1 (Kohlhofer and Penny, 1996). The Johnson-cook model parameters of coatings are from Ref. (Johnson and Cook, 1983). Thermophysical properties of WC-Co cermet is shown in Table 2 (Clough *et al*., 2003).

Explicit model: A two-dimensional axisymmetric model of a 30 μm diameter WC-Co particle impacting on an AISI 1045 substrate disc of 1 mm radius and 1 mm thickness was generated using ABAQUS version 6.10. A dynamic,

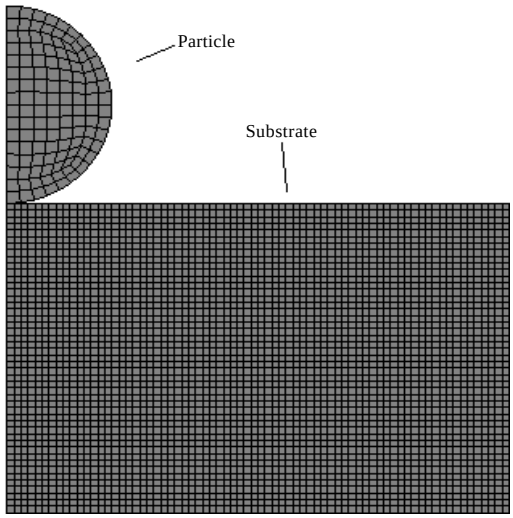

Fig. 2: Axisymmetric model of SS 316 particle impact on an SS 316 substrate

Table 2: Thermophysical property of WC-Co

Density (kg mm^{-3})	14320
Solidus temperature (K)	1580.0
Liquidus temperature (K)	1640.0
Melting point (K)	1768.0
Specific heat (J kg^{-1} K^{-1})	295.0
Young's modulus (GPa)	331.0
Poisson's ratio	0.25
Latent heat (J kg^{-1})	420.000

explicit temperature-displacement coupled analysis was carried out to study the high strain-rate impact process using ABAQUS/Explicit. In the model, spray conditions were characterized by the particle velocity and temperature. These parameters were considered as the key variables in the FE model and analysis were performed in different velocities.

Four-node linear displacement and temperature elements were used to discretize the particle and the substrate. All the displacements on the bottom face of the substrate were restrained. Symmetry boundary conditions were used on the left-hand side of the model. Upon impact, the sprayed particle deforms and spreads over the substrate, forming a splat. The FE analysis assumes that, after first contact, the particle remains attached to the substrate. This was implemented by assigning a no-separation criterion between the contacting nodes of the impinging particle and the underlying substrate. Figure 2 illustrates the axisymmetric FE model of an impinging particle on the substrate.

The particle starts to deform immediately after impact, causing the formation of a crater on the substrate. In the early stage of the impingement (50 nsec), the deformation

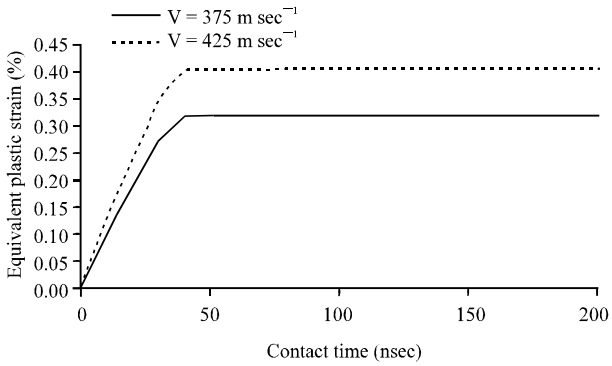

Fig. 3: FE-predicted effective plastic strain during impact

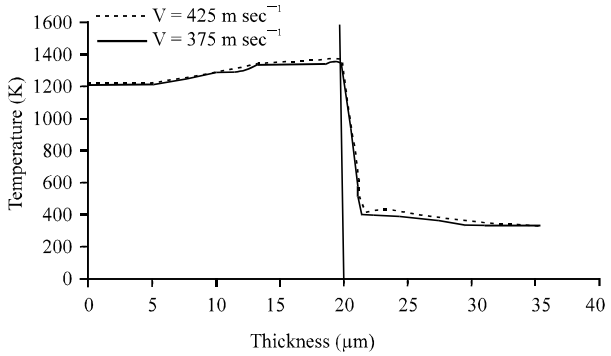

Fig. 4: FE-predicted temperature distribution across the splat and the substrate thickness after the impact (T = 1260 K)

of the contact surface is evident. At 100 nsec, when the particle kinetic energy has fallen to zero, the particle flattens to final shape.

Figure 3 illustrates the FE-predicted change in effective plastic strain in splat during impact. It clearly shows that regardless of particle velocity, after 50 nsec there is not considerable change in splat deformation. However, it was predicted that the higher the particle velocity the greater plastic deformation.

In this study, it was assumed that 90% of the inelastic energy generated during impact was dissipated as heat. At the substrate-splat interface significant temperature increase is observed as a result of kinetic energy being converted to internal energy and part of it to plastic deformation. Figure 4 describes the predicted temperature distribution across the splat and the substrate thickness 100 nsec after initial contact. An increase of approximately 130 K is predicted in the particle upon impact in 375 m sec^{-1}. The impact process also imposes extra heat to the substrate and is predicted to affect a region up to about 40 μm deep. A greater temperature rise is predicted in the substrate along the

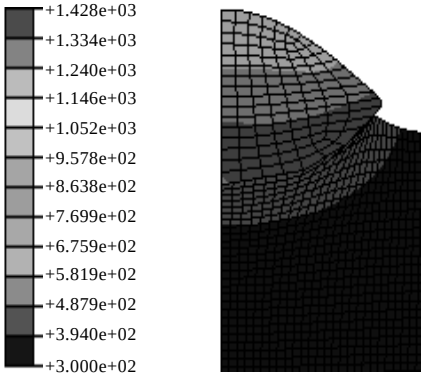

Fig. 5: Temperature contours on the splat and substrate 100 nsec after impact

particle-substrate interface when particles are sprayed at 425 m sec^{-1}. In this region, the temperature rises to 1345 K at 100 nsec.

The temperature contours from sprayed splats having a temperature of 1200 K, landing at 425 m sec^{-1} is presented in Fig. 5 for impact time of 100 nsec. The temperature contours on the substrate surface indicate that the temperature increase in substrate is much lower than that of the particle which is attributed to the smaller plastic deformation experienced by the substrate during impact.

Adhesion and rebound energy: The impact processes consist of an elastic-plastic loading followed by an elastic unloading during which the elastic recovery occurs. The essential energy for bouncing the particle from the substrate during the unloading is defined as the rebound energy in the impact process of high velocity oxy fuel spraying. Referring to the drop-ball dynamic hardness test the rebound energy (R) is expressed as:

$$R = \frac{1}{2} e_r m_p v_p^2 \quad (4)$$

where, the recoil coefficient e_r for spherical particles is given by:

$$e_r = 11.47\left(\frac{\bar{\sigma}_Y}{E^*}\right)\left(\frac{\rho_p v^2_p}{\bar{\sigma}_Y}\right)^{-1/4} \quad (5)$$

$$E^* = \frac{1-\nu^2_s}{E_s} + \frac{1-\nu^2_p}{E_p} \quad (6)$$

where, m_p and v_p are the mass and velocity of impact particle, $\bar{\sigma}_Y$ is the effective yield stress during the impact,

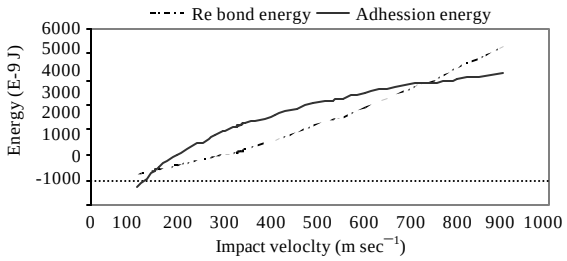

Fig. 6: The comparison of the adhesion energy with the rebound energy of individual particle

E* is the Equivalent elastic modulus of the powder and substrate materials and ρ_p is the density of the particle material. Note that shockwave effects and adiabatic heating can complicate the impact process. A strain-hardening, strain rate sensitive, thermal-softening and deformation localization must be considered for the calculation of the effective yield stress $\bar{\sigma}_Y$ which is provided from the Johnson-Cook plasticity model.

Adhesion behaviors during supersonic impingement are important for particle deposition and coating build-up in HVOF spray technologies. The adhesion energy (A) which is defined as the energy for detaching the bonded particle from the substrate, is expressed as (Kurochkin *et al*., 2002):

$$A = a\% A_{max} \quad (7)$$

where, A_{max} is the maximum adhesion energy of a given particle to the substrate; a% is the fraction of bonded atoms per unit adhesive interface and is also called the relative strength of the bond between the particle and substrate. In previous research that investigated interactions during Detonation Gun spraying, Shorshorov and Kharlamov (1987) developed a relation for the fraction of bonded atoms during impact. Kurochkin *et al*. (2002) improved this relation for the kinetic spraying process and reported their expression. This relation is not shown here for briefness. The contact time in this model selected to be 100 nsec and contact surface calculated from the indent generated 100 nsec after contact.

The competition of rebound and adhesion energy: In thermal and kinetic spraying processes, the particle is assumed to bond onto the substrate when the adhesion energy (A) is greater than the rebound energy (R). The comparison of the adhesion energy with the rebound energy of individual particle impact is shown in Fig. 6. When the particle velocity is low, the adhesion energy is

Table 3: Critical particle velocities in developed model

T_p	V_{opt}	V_{max}	V_{min}
	----------m sec^{-1}----------		
1620 K	400	735	150

lower than the rebound energy, so then the particles cannot be deposited on substrate surface. When the particle velocity achieved a threshold value (150-200 m sec^{-1}), the adhesion energy started to increase. When the particle velocity is high enough for the adhesion energy to exceed the rebound energy, particle attachment is obtained.

The particle velocity where the curves of the two energies intersect is the minimum velocity for individual particle deposition onto the substrate. In our calculations, another point where the energy curves intersect was obtained which is called the maximum velocity for the particle deposition onto the substrate. When the particle velocity was higher than this point, the adhesion energy was below the rebound energy and the splat could not attach onto the substrate.

In individual particle impingement processes, the deposition characteristics were a result of the opposition between the adhesion energy and rebound energy which were affected by the impact temperature and velocity of impact and the material properties of the particle and substrate. The occurrence of a rebound phenomenon was also dependent on the material properties of the powder and substrate. When the two curves meet one time, the particle could bond onto the substrate after it reached the critical velocity for its deposition. When the adhesion and rebound energy meet more than one time, the rebound phenomenon could be observed at higher velocities. Because of the rebound phenomenon, a definite range of impact velocities is introduces for optimum deposition condition. An optimum impact velocity for maximum deposition efficiency is at the peak value of difference between adhesion and the rebound energy. The results are concluded in Table 3.

CONCLUSION

A two-dimensional axisymmetric model of a 30 μm diameter WC-Co particle impacting on an AISI 1045 substrate was developed. The bonding and rebounding energies have been compared. The critical velocities also were obtained. The optimum velocity was predicted to be 400 m sec^{-1} for particle of 30 μm diameter.

ACKNOWLEDGMENT

The authors gratefully acknowledge the financial support by the Islamic Azad University, Ahwaz branch for this research program.

REFERENCES

Ahmad, I., S.A. Ali and Barkatullah, 2007. Elements of an effective repair program for cavitation damages in hydraulic turbines. Inform. Technol. J., 6: 1276-1281.

Assadi, H., F. Gartner, T. Stoltenhoff and H. Kreye, 2003. Bonding mechanism in cold gas spraying. Act Mater., 51: 4379-4394.

Bansal, P., P.H. Shipway and S.B. Leen, 2006. Effect of particle impact on residual stress development in HVOF sprayed coatings. J. Therm. Spray Technol., 15: 570-575.

Cherigui, M., A. Hebbar, N.E. Fenineche and C. Coddet, 2007. Modelling of magnetic proprieties of FeNb coatings produced by HVOF thermal spraying. J. Applied Sci., 7: 386-391.

Clough, R.B., S.C. Webb and R.W. Armstrong, 2003. Dynamic hardness measurements using a dropped ball: with application to 1018 steel. Mater. Sci. Eng. A, 360: 396-407.

Dykhuizen, R.C., M.F. Smith, D.L. Gilmore, R.A. Neiser, X. Jiang and S. Sampath, 1999. Impact of high velocity cold spray particles. J. Therm. Spray Technol., 8: 559-567.

Gilmore, D.L., R.C. Dykhuizen, R.A. Neiser, T.J. Roemer and M.F. Smith, 1999. Particle velocity and deposition efficiency in cold spraying. J. Therm. Spray Technol., 8: 576-586.

Grujicic, M., J.R. Saylor, D.E. Beasley, W.S. De-Rosset and D. Helfritch, 2003. Computational analysis of the interfacial bonding between feed powder particles and the substrate in the cold-gas dynamic-spray process. Applied Surf. Sci., 219: 211-227.

Hutchings, I.M., 1981. A model for the erosion of metals by spherical particles at normal incidence. Wear, 70: 269-281.

Johnson, G.R. and W.H. Cook, 1983. A constitutive model and data for metals subjected to large strains, high strain rates and high temperatures. Proceedings of the 7th International Symposium on Ballistics, April 19-21, 1983, The Hague, Netherlands, pp: 541-547.

Kamnis, S. and S. Gu, 2005. Numerical modelling of droplet impingement. J. Phys. D: Applied Phys., 38: 3664-3673.

Kamnis, S., S. Gu, T.J. Lu and C. Chen, 2008. Numerical modelling of sequential droplet impingements. J. Phys. D: Applied Phys., Vol. 41. 10.1088/0022-3727/41/16/165303.

Karni, M., A. Fartaj, G. Rankin, D. Vanderwet, W. Birtch and J. Villafuerte, 2006. Numerical simulation of the cold gas dynamic spray process. J. Therm. Spray Technol., 15: 518-523.

Kohlhofer, W. and R.K. Penny, 1996. Hardness testing as a means for creep assessment. Int. J. Press. Ves. Pip., 66: 333-339.

Kurochkin, Y.V., Y.N. Demin and S.I. Soldatenknov, 2002. Demonstration of the method of cold gasdynamic spraying of coatings. Chem. Petrol. Eng., 38: 245-248.

Li, C.J. and W.Y. Li, 2003. Deposition characteristics of titanium coating in cold spraying. Surf. Coat. Technol., 167: 278-283.

Lyphout, C., P. Nyle'n, A. Manescu and T. Pirling, 2008. Residual stresses distribution through Thick HVOF Sprayed Inconel 718 coatings. J. Therm. Spray Technol., 17: 915-923.

Sahraoui, T., S. Guessasma, M.A. Jeridane and M. Hadji, 2010. HVOF sprayed WC-Co coatings: Microstructure, mechanical properties and friction moment prediction. Mat. Des., 31: 1431-1437.

Santana, Y.Y., P.O. Renault, M. Sebastiani, J.G. La-Barberaa and J. Lesaged *et al*., 2008. Characterization and residual stresses of WC-Co thermally sprayed coatings. Surf. Coat. Technol., 202: 4560-4565.

Shorshorov, M.K. and Y.A. Kharlamov, 1987. Physical and Chemical Principles of Detonation Gas Spray Coating. Nauka Publishing, Moscow, Russia.

Sohi, M.H. and F. Ghadami, 2010. Comparative tribological study of air plasma sprayed WC?12%Co coating versus conventional hard chromium electrodeposit. Tribol. Int., 43: 882-886.

Souiyah, M., A. Muchtar, A. Alshoaibi and A.K. Ariffin, 2009. Finite element analysis of the crack propagation for solid materials. Am. J. Applied Sci., 6: 1396-1402.